

Suitability of radiochromic medium for real-time optical measurements of ionizing radiation dose

Alexandra Rink,^{a)} I. Alex Vitkin, and David A. Jaffray

Princess Margaret Hospital/Ontario Cancer Institute, Department of Medical Biophysics and Radiation Oncology, University of Toronto, Toronto, Ontario M5G 2M9, Canada

(Received 12 October 2004; revised 20 December 2004; accepted for publication 2 February 2005; published 29 March 2005)

A system, consisting of a novel optical fiber-based readout configuration and model-based method, has been developed to test suitability of a certain radiochromic medium for real-time measurements of ionizing radiation dose. Using this system with the radiochromic film allowed dose measurements to be performed during, and immediately after, exposure. The rates of change in OD before, during, and after exposure differ, and the change in OD during exposure was found to be proportional to applied dose in the tested range of 0–4 Gy. Estimating applied dose within an average error of less than 5% did not require a waiting time of 24–48 h as generally recommended with this radiochromic film. The errors can be further reduced by performing a calibration for each individual dosimeter setup instead of relying on batch calibration. Measurements of change in OD were found to be independent of dose-rate in the 95–570 cGy/min range for applied dose of 1 Gy or less. Some error was introduced due to dose-rate variation for doses of 2 Gy and above. The major limiting factor in utilizing this radiation sensitive medium for real-time *in vivo* dosimetry is the strong dependence on temperature in the clinically relevant range of 20–38 °C. © 2005 American Association of Physicists in Medicine. [DOI: 10.1118/1.1877832]

I. INTRODUCTION

Approximately 50% of cancer patients receive either external or internal radiation therapy for management of their disease. The International Commission of Radiation Units (ICRU) recommends treating patients with ionizing radiation dose within 5% of the total prescribed dose; both the prescribed dose and the accuracy of delivery are vital if therapy is to be successful.¹ Currently, the majority of external treatments are divided into fractions, delivered daily over several weeks. In the past years, treatments have become more conformal due to implementation of intensity modulated radiation therapy and image-guided radiation therapy. With the development of these new technologies, a trend has been evolving toward higher target absorbed dose values, fewer fractions, smaller treatment volumes, and steeper dose gradients, increasing chances of missing part of tumor due to incorrect dose calculation. Dose calculation algorithms can produce systematic errors (>10%) in regions where electron equilibrium is not established (near air cavities, bone or prosthetic implants) even when patient's anatomy, geometry, and organ densities are taken into consideration.² Accurate assessment of the dose distribution in such regions is vital to rapid innovation and development of new radiation therapy technologies and techniques, and can be verified by performing dose measurements.

Dose calculations for internal radiation therapy (brachytherapy) can be just as, if not more, complicated as many small sources are used and electron equilibrium is often not achieved. Furthermore, the ionizing radiation dose and dose rate at a given point is largely dependent on the distance from the radioactive seeds, yielding steep dose gradients and largely varying dose rates. As in the case of external radiation therapy, accurate assessment of the dose distribution in

brachytherapy treatment would allow for better informed and quicker development of new therapy techniques.

A dosimeter that can be used across a wide range of energies could be implemented in both external beam radiation therapy and brachytherapy, simplifying the dosimetric procedures to just one device. Such a dosimeter could also be used during various diagnostic and positioning procedures. New technologies, such as cone-beam computed tomography used in image-guided therapy, often require dosimetric studies before protocols using that technology can be approved and implemented. Accurate assessment of the dose given to the patient using a reliable dosimeter with a water-equivalent response would save time and money over using multiple dosimeters with a significant over- or under-response to low energy x rays and inferring the dose via several correction factors and calculations.

A list of requirements in choosing an *in vivo* dosimeter is given in Table I, and can be used as a scheme for evaluation. The goal of these investigations is to develop a dosimeter that is economically and logistically acceptable (low-cost, disposable, reusable, and sterilizable). To meet these requirements, a water equivalent dosimeter which undergoes an immediate change in optical properties upon exposure to ionizing radiation is proposed. The difference in a particular quantitative optical property is to be measured via optical fibers, and ionizing radiation dose is to be inferred through a calibration model. In the initial embodiment of the device, the radiation sensitive material present in GafChromic® MD-55 radiochromic film was investigated for suitability in the application of external beam patient dosimetry.

Review of GafChromic MD-55. To better understand the results presented in this paper, the reader is provided with a review of literature and explanation of solid-state polymer-

TABLE I. List of criteria of *in vivo* point-based real-time dosimeter.

| Criterion No. | Criterion | Comments |
|---------------|--|---|
| 1 | small size ³ ($<1 \text{ mm}^3$) | Does not physically perturb tissue and effect delivered dose to surrounding tissue; can measure point dose at interfaces between tissues of varying densities and composition; used on steep part of dose–depth curve or in the penumbra region; no build-up required for measurement |
| 2 | Near water-equivalent ^a (difference $<10\%$) (response independent of energy) | Does not alter dose distribution to tissue (tissue assumed to be similar to water); ^a own reading converted to dose delivered to water (and/or tissue); does not cause artifacts during low-energy image guidance (for IGRT) |
| 3 | Fast kinetics and stable response (interrogation process does not induce false signal) | Both required for real-time readout of dose |
| 4 | Signal \propto dose in 1–1000 cGy range (linear within 2%) | Simplicity of conversion from measurements to dose; no need to track delivered dose to-date; simple function is acceptable in lieu of linearity |
| 5 | Dose resolution (down to cGy) | Measurements of doses down to a few cGy with relatively small errors (few %); suitable for IMRT |
| 6 | Dose-rate independence (10–1000 cGy/min) (no statistical difference using $\alpha=0.05$) | No need for prior knowledge of dose; simplicity of measurements throughout the body |
| 7 | Insensitive to environmental conditions ($<2\%$ variation over clinical temperature range of 20–38 °C) | Temperature, humidity, and light insensitivity allows for easier incorporation and use within clinic |
| 8 | Nontoxic | Requirements of dosimeter embodiments are relaxed when medium contained within is nontoxic |

^aReference 3

ization. An understanding of the process that forms the basis for radiochromic dosimetry is required if the real-time dosimetry system is to be quantified and optimized. The time course of the energy transfer and subsequent processes that lead to changes in optical density are also important for rational design.

General experience. Radiochromic films have been used for nearly 30 years in the field of dosimetry.⁴ Commercially available radiochromic dosimeters are manufactured by International Specialty Products (ISP), and some are sold under the product name of GafChromic MD-55. A broad assessment of its characteristics suggests that it is a good candidate for the proposed point-based dosimeter: the sensitive medium from GafChromic MD-55 film can be packaged as a small volume placed at the tip of an optical fiber (closed system to minimize any interference from the tissue, such as humidity); it has response characteristics within 5% of water and striated muscle for photons of energy in the range of 0.1–10 MeV, and electrons in range of 0.01–30 MeV.⁵

Upon exposure to heat, ultraviolet (UV) light, and high-energy photons and electrons, the monomers polymerize to provide an absorbance spectrum with two peaks (675 and 615 nm), creating a polymer with a blue tint.^{5–7} The third requirement appears to have also been met, since the change in absorbance is a linear function of the absorbed dose,⁸ although the dynamic range of this function depends on the

wavelength at which the measurements are obtained.^{9–13} The film has been reported to resolve dose to 1.5 Gy with a precision of 5% or better, using the 671 nm absorption peak [ISP Corp. product information], and this resolution can be further increased by increasing the thickness of sensitive layer.¹⁴ The requirement of real-time readout appears to be a significant impediment to use of GafChromic MD-55 film. Time frames of 24–48 h after exposure are recommended. Additional investigations are required to resolve this issue.

Less than 5% difference in net change in absorbance of GafChromic MD-55 film exposed to 10 Gy at dose rates of 0.034–3.422 Gy/min is expected [ISP Corp. product information]. However, validity of the measurements done with this film has been questioned for low dose-rate brachytherapy. Ali *et al.* (2003) reported the kinetics of film darkening as a function of post-exposure time depends on the total dose, with the development being faster at the lower doses.¹⁵ These findings are a concern for real-time dosimetry and require further investigation. While the focus of this study is to apply the dosimeter in the context of external beam radiotherapy, where dose rates are typically greater than those in brachytherapy, a range of doses and dose rates, over which post-exposure development from the first few fractions of the treatment does not introduce error in the absorbance reading and final dose estimate, should be clearly defined.

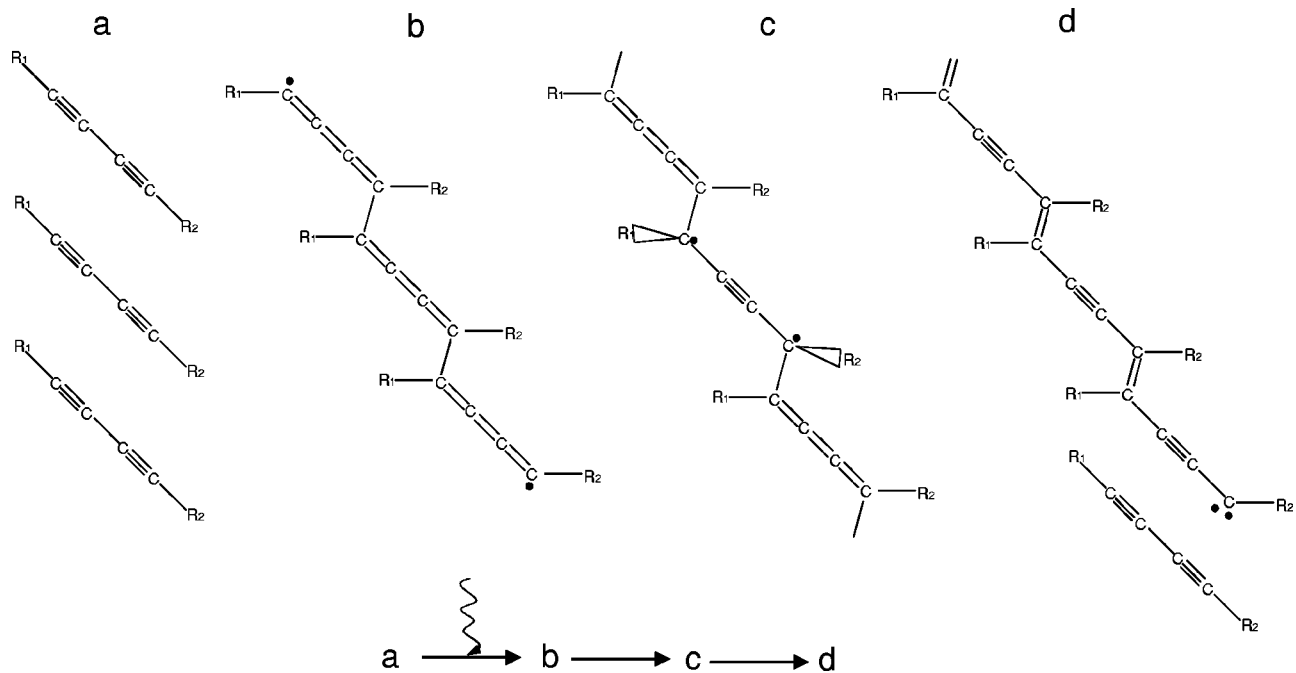


FIG. 1. (a) Diacetylene monomers, upon exposure to ionizing radiation, polymerizes into (b) butatriene structure polymer; as the polymer chain grows, it rearranges via (c) an intermediate between butatriene structure and acetylene structure, into (d) acetylene structure polymer.

McLaughlin *et al.* (1996) reported that propagation of the polymerization is complete within 2 ms of a single 20 Gy 50 ns pulse.⁷ It is unclear, however, if the polymerization occurred mostly due to ionizing radiation or heat. The literature describes a continuous increase in absorbance even after irradiation is complete,^{16,17} with the absorbance being a function of a logarithm of elapsed time.¹⁸ Hence, it has generally been recommended to perform the measurements 24 h⁵ to 48 h later¹⁸ by both researchers and manufacturers (ISP Corp. product information). Measurements are further complicated by the shift in wavelength of maximum absorbance (λ_{\max}) to lower wavelengths as dose increases.^{5,9,16,17}

GafChromic MD-55 film is stable during storage or short exposures to ambient light,¹⁹ satisfying part of a seventh requirement of *in vivo* dosimeter. However, the temperature dependence of absorbance of GafChromic MD-55 is complicated, and humidity and pressure dependence poorly documented. Increase in temperature during irradiation was reported to correspond to a decrease in absorbance and a peak shift to lower λ ($\lambda_{\max}=677.5$ nm at 18.6 °C, 673 nm at 28.0 °C for 6.9 Gy),^{5,18} with the latter effect being reversible if temperature fluctuations occur during measurement, not irradiation.⁵ Others report an increase in absorbance with an increase in temperature.^{16,20} This discrepancy is likely due to a choice of wavelength for absorbance measurements, as the λ_{\max} depends on temperature, and also due to a range of temperatures sampled. It has been shown that a He-Ne laser operating as low as 0.1 mW will cause an increase in absorbance of GafChromic MD-55 in 5 min, with this effect being stronger for films exposed to smaller doses.²¹ For this reason, the absorbance measurements should be performed using low optical powers to prevent polymerization due to the heat

produced by the light. Above 60 °C, the color of the film changes from blue to red, as the crystals melt.⁷ Chu *et al.* (1990) reported a dependence of GafChromic MD-55 absorbance on the relative humidity, with the increase from 35% to 100% humidity resulting in a decrease in sensitivity by approximately 14% when irradiated to 5–40 kGy.¹⁶ No similar data have been published to date for doses of relevance to external radiation therapy.

The crystal suspension used in GafChromic MD-55 film is hazardous if ingested, inhaled, or absorbed through skin,²² although it would not be present in a substantial enough amount within the point-based dosimeter to do damage to the patient.

Overall, GafChromic MD-55 is a stable, well-performing dosimeter medium, that meets several of the requirements for the proposed *in vivo* dosimeter system. However, most of the published literature applies to measurements performed 24–48 h post-exposure, and may not hold true during or immediately after exposure. Additional investigations are required to evaluate the performance of GafChromic MD-55 for real-time dose measurements. These investigations are performed using the novel optical fiber-based system described in the following.

Solid-state polymerization of diacetylenes. The active component of GafChromic MD-55 radiochromic film is a double-substituted diacetylene monomer with one polar end,²² organized into a crystal [Fig. 1(a)].^{5,18} The packing of the monomers within the crystal lattice depends on the type and size of the side groups (R_1 and R_2).^{23,24} Generally, for polymerization to occur, the monomers should be packed such that the triple bonds of adjacent monomers are within an approximate distance of 0.4 nm or less.²⁵ It has been

shown that a diacetylene monomer similar to that in GafChromic MD-55, upon exposure to heat, x rays, γ rays, or photons in the UV region, polymerizes into a butatriene structure polymer [Fig. 1(b)].²⁶ For this particular monomer, this structure is stable in short chains (i.e., $n \leq 6$). Once the polymer chains propagate longer ($n > 6$), polydiacetylene undergoes reformation via an intermediate [Fig. 1(c)] into an acetylene structure [Fig. 1(d)] with a carbene (carbon atom with two unpaired electrons) at each end of the chain. The acetylene structure is of a lower energy configuration,²⁶ and any additional monomer will attach to the chain with a double bond.

The solid-state polymerization of GafChromic MD-55 and other similar diacetylene monomer crystals is *topotactic*, where the reaction proceeds along one axis of the crystal, but not in the perpendicular axes.²⁵ The individual chains, once randomly initialized²⁷ by energy transferred from ionizing particles or scattered photons, grow independently of each other.²⁵ As the polymer increases in units, the absorbance of the polymer–monomer mixture increases due to an increase in the double-bond concentration between the units.²⁸ The shape of the absorbance spectrum is very similar to that of GafChromic MD-55 film and is said to be typical of a guest diacetylene polymer in a monomer crystal.^{26,28}

The structure of a diacetylene polymer is often slightly different than that of the crystalline monomer chain due to tilting of each unit with polymerization.²⁵ Initially, the crystal structure of the polymer is controlled by the crystal structure of the surrounding monomer.²⁵ Once the local polymer concentration increases and the crystal structure of the monomer can no longer produce enough strain to control the polymer structure, the polymer chains will reorganize into a lower energy arrangement. A transition in the structure of the diacetylene backbone is believed to be accompanied by a shift in the absorption peaks, and by a change in length of polymer chain.²⁹ This explains the shift of the absorption peak with increased dose.^{5,9,16,17} In the case of GafChromic MD-55, the polymer structure is shorter, and as the chain grows, it contracts.^{22(b)} Hence, the space between the last monomer unit in a chain and the next monomer unit increases as the polymerization proceeds. In order for polymerization reaction to proceed to the end of monomer chain, any mismatch of monomer and polymer must not lead to large spatial separation between the two phases.²³ However, with increasing concentration of polymers, the crystal structure required for polymerization is disturbed, and the number of units in a polymer chain per amount of energy deposited decreases as polymerization proceeds. Generally, the carbenes on both ends of the chain will continue to react until they reach an impurity that inhibits or significantly slows further polymerization,²⁷ or they terminate polymerization upon interaction with another carbene.³⁰ Since GafChromic MD-55 is $\sim 99\%$ free of chemical impurities,^{22(b)} the impurity lies in the form of a large separation between the polymer chain and the adjacent free monomer.

It is expected that most of the energy is transferred to surrounding media (monomer crystals) within 10^{-3} s of a

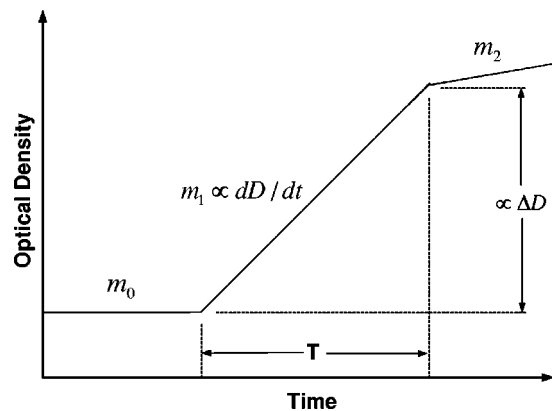


FIG. 2. A model of optical density of GafChromic MD-55 vs time before, during, and after exposure. The irradiation is applied for a period of time T . The change in optical density during exposure is proportional to applied dose.

passage of high-energy electron.³¹ The transferred energy would initiate polymerization within the monomer crystal. For a diacetylene monomer crystal similar to that in GafChromic MD-55, it has been reported that the butatriene-to-acetylene phase-transition occurs over a period of 4 h at the temperature of 100 K.²⁶ It is reasonable to believe that the rate of phase transition at ~ 23 °C is much higher, and possibly nearly instantaneous.²⁷ Although carbenes are unstable and highly reactive species³⁰ and carbene reactions generally have high reaction rates, the reactivity of diacetylene monomers is a function of their spatial arrangement within the lattice.^{23,24} Since the distance between monomers grows as the polymerization proceeds due to chain contraction, the reactivity of each new monomer to the polymer chain decreases; therefore, the kinetics of such a diacetylene polymerization within monomer crystals is not constant. At some point during the polymerization, the energy of the carbenes on the end of the chain is not sufficient to overcome the energy barrier created by the large distance to the next free monomer, and the probability of adding another monomer to the polymer drastically decreases. Nonetheless, a large percentage of an increase in absorbance would occur during exposure, and is referred to from now on as *intra-exposure growth*. The polymerization reaction appears as if the crystal is heavily doped.⁷ Carbenes that continue to react after the exposure has completed, contribute less than 20% to the overall change in absorbance [ISP Corp. product information], producing postexposure, or *inter-exposure*, development. This inter-exposure growth in change in OD (ΔOD) is asymptotic in nature.¹⁸

As shown in Fig. 2, the rate of intra-exposure ΔOD is proportional to the dose rate, and the net change in ΔOD is therefore proportional to absorbed dose. This model should hold true assuming the dose is small and the dose rate is large, such that the polymer concentration is not sufficiently high enough to decrease polymerization kinetics for the subsequent dose fractions. For larger delivered doses, or for doses delivered at low dose rates, the inter-exposure development from each deposition of dose will introduce errors to

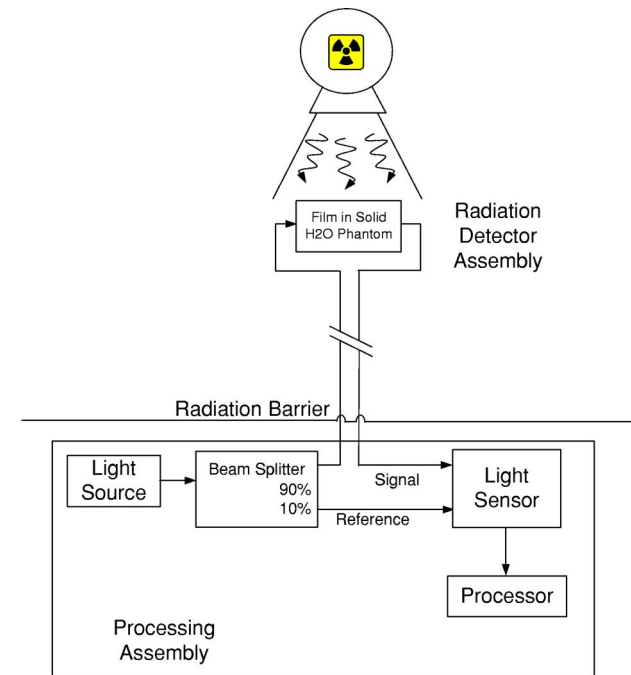
dose estimates due to the above-discussed reasons. To test the model shown in Fig. 2, a system and method that enables measurements during exposure is needed.

The use of optical fibers for remote dosimetry has been previously reported on,^{32,33} including systems that work by monitoring the degree of radiation-induced absorption within the fiber.^{34,35} We report a novel fiber-based optical readout configuration that enables a medium, such as GafChromic MD-55 film, to be evaluated for suitability in a real time point-based dose measurement system. The described dosimetry system, including optical readout configuration and method, exploits the intra-exposure changes in OD within radiochromic medium to estimate radiation doses in real time, where dose measurements would generally be performed 48 h after exposure using conventional methods. The system contains no metallic components near point of measurement. This approach permits water-equivalent dosimetry in small sensitive volumes over a large range of energies, dose rates, and doses; such a system can be used as a platform for testing other dosimetric media. The system is used to evaluate the sensitive medium employed in GafChromic MD-55 with respect to the eight requirements of the above-described “ideal” dosimeter.

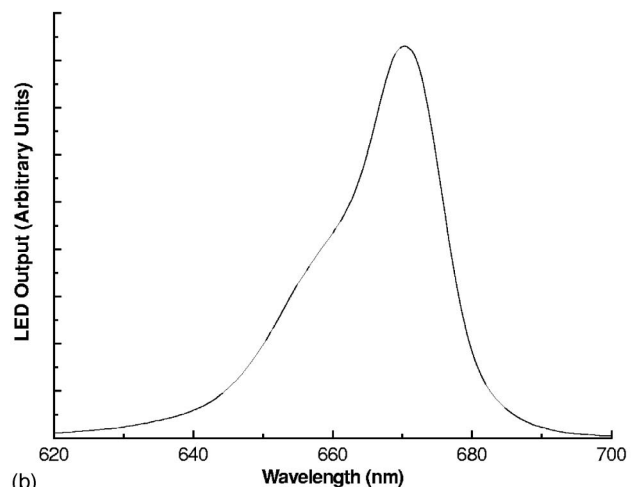
II. METHODS AND MATERIALS

The optical dosimetry system is schematically illustrated in Fig. 3(a). Since the main focus of this paper is the real time behavior of GafChromic MD-55 film, no considerable amount of time was spent in perfecting the design of the optical system. A Roithner Lasertechnik (Vienna, Austria) light-emitting diode (LED), with peak emission wavelength of 670 nm [Fig. 3(b)], was chosen as the light source to provide the greatest sensitivity^{12,13} and eliminate any unnecessary light that may heat the sample, thus altering measurements.²¹ It was connected to a multimode optical fiber (600/630 core/cladding diameters in μm) leading to an OZ Optics Ltd. (Carp, Ontario, Canada) nonpolarizing 90:10 (sample:reference at 680 nm) beam splitter. The sample beam traveled through 17 m of fused silica fiber (600/630 core/cladding) to delivery fiber, which illuminated a spot $\sim 650 \mu\text{m}$ in diameter of a 1 cm \times 1 cm piece of GafChromic MD-55 film contained within a cylindrical Solid Water™ phantom [Figs. 4(a)–4(d)]. The dimensions of fused silica delivery and collection fibers are shown in Fig. 4(d).

The phantom was designed to allow easy replacement of film, to provide electron equilibrium at the point of measurement, located at the center of the phantom, and to allow for easy calculation of dose delivered to the point of measurement by using peak scatter factor for the linear accelerator on which exposures were performed.³⁶ The air gaps within the film holder and phantom were kept to a minimum: sufficient space to place the film, and small cylindrical spaces to allow passage of interrogating light to the film as well as collection of most of the light transmitted. The scattering was assumed to be negligible, and the fraction of light reflected was assumed to be independent of dose. A recent study by Fusi *et al.* (2004) confirmed that in the 600–700 nm region, the ab-



(a)



(b)

FIG. 3. (a) Schematic of experimental setup. Detector is an Ocean Optics Inc. SD2000 dual-channel spectrophotometer. Processor is a computer with Ocean Optics Inc. IOBase32 and Matlab® 6.1. (b) Emission spectrum of the LED as detected by the spectrophotometer.

sorption coefficient of GafChromic MD-55 film is larger than the scattering coefficient. On the other hand, they showed that total reflectance decreased from $\sim 14\%$ to $\sim 9\%$ over 0–4 Gy range.³⁷ However, no corrections were performed on our data in light of this information.

Light transmitted through the film returned via another 17 m (same as above) of optical fiber into the signal channel of a spectrophotometer (Ocean Optics Inc., Dunedin, FL; SD2000 dual-channel, 12 bit analog-to-digital converter). The 10% reference beam was attenuated using 2.00 OD neutral density filter (Melles Griot, Carlsbad, CA), and was monitored on the second spectrophotometer channel to measure fluctuations in the output light during evaluation of ef-

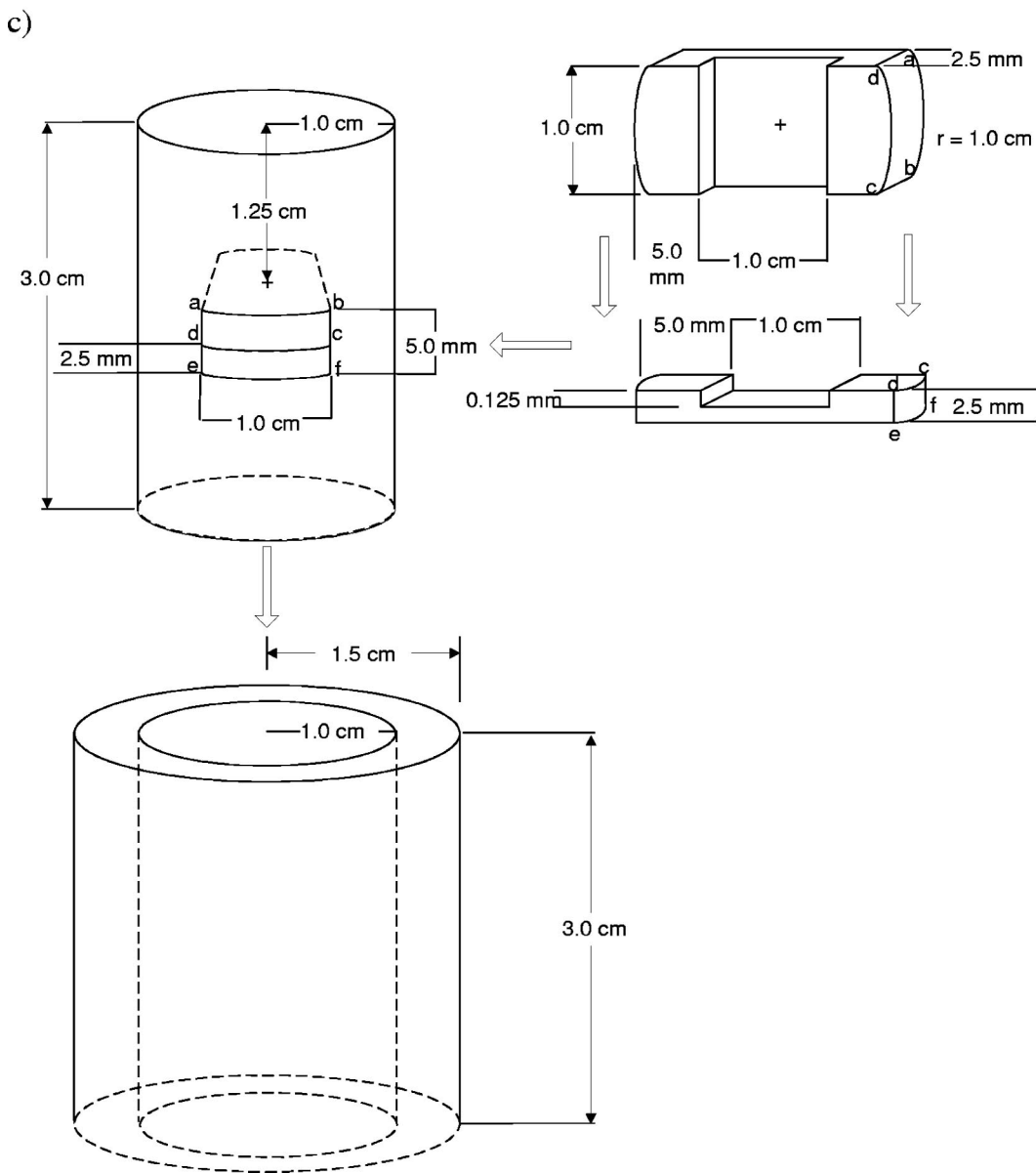
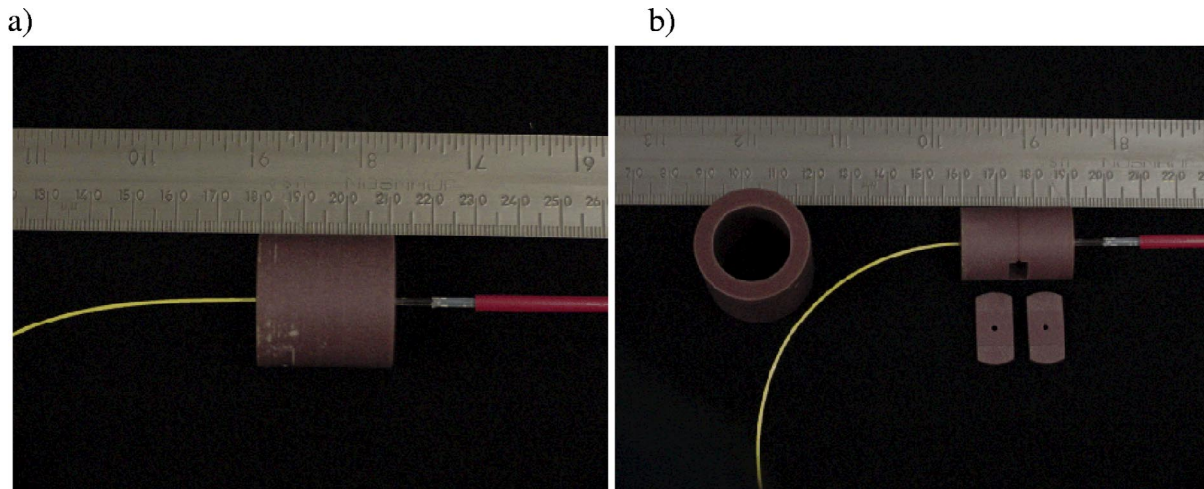


Fig. 4. Solid Water™ phantom (a) assembled, (b) disassembled, (c) schematic. (d) Schematic of cross section of film holder in Solid Water™ phantom. The light emitted from delivery fibers illuminates a spot on the GafChromic MD-55 film ~650 μm in diameter.

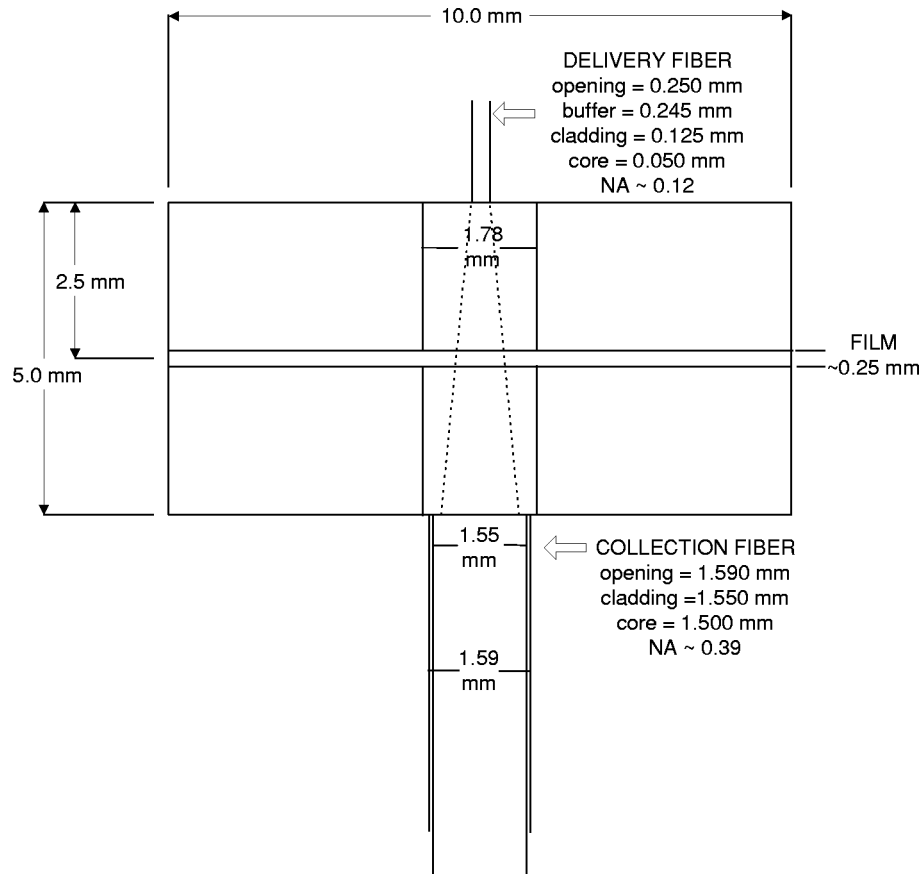


Fig. 4. (Continued).

fect of light on OD of film (described in detail in the following). The spectrometer software used was Ocean Optics Inc. OOIBase32™ (Dunedin, FL), and data were processed with MATLAB® v6.1 (Natick, MA).

Briefly, the system operated with 30 mA power supply driving light output from the LED. Spectra were collected starting 5–10 s prior to the commencement of exposure. The spectrometer integration time ranged from 125 to 750 ms, depending on the study performed. For integration time <500 ms, the spectra were captured no faster than 2 Hz. The change in absorbance (ΔA) for each wavelength was calculated using

$$\Delta A(\lambda) \equiv \log_{10} \left(\frac{I_{0s}(\lambda) - I_D(\lambda)}{I_s(\lambda) - I_D(\lambda)} \right), \quad (1)$$

where I_{0s} is the average intensity of five spectra (taken before the beam is turned on), I_s is the sample light intensity at some point in time, and I_D is the dark signal. I_D is defined as the average of the signal obtained over a period of 15 min without a light source. Figure 5 shows the change in absorbance of a single piece of GafChromic MD-55 prior to exposure, immediately after exposure to 381 cGy at 286 cGy/min, and at several intervals after the completion of exposure. The spectral “window” of interest, or range for optical density calculation, is a 10 nm window below the

main peak (670–680 nm). This window was chosen to minimize the errors due to shifting of wavelength of maximum absorbance with dose,^{5,9,16,17} yet still provide a high sensitivity.¹³ The change in optical density (ΔOD) was then defined as

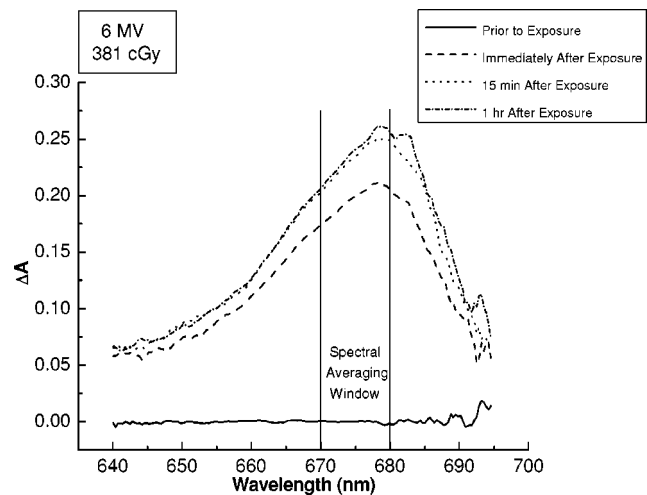


FIG. 5. Change in absorbance of GafChromic MD-55 film at various wavelengths plotted before exposure, immediately after end of exposure, and 15 and 60 min after the end of exposure.

$$\Delta OD \equiv \frac{1}{\lambda_1 - \lambda_n} \times \sum_{i=1}^{n-1} \left(\frac{\Delta A_i + \Delta A_{i+1}}{2} \right) \times (\lambda_i - \lambda_{i+1}), \quad (2)$$

where λ_1 to λ_n are wavelengths that span the window of interest in the spectrum. The range of integration times and the range of wavelengths chosen yielded an average signal-to-noise ratio of nearly 800 in the ΔA absorbance spectrum.

One approach is to limit the objective to determination of applied dose at the end of a beam segment. This approach overcomes the inter-exposure time dependence of OD on various parameters discussed earlier by measuring the ΔOD at the end of exposure. According to the model in Fig. 2, this event is marked by an abrupt change in ΔOD increase, and can be assumed to occur when the $\delta OD / \delta t$ is half of the average $(\delta OD / \delta t)_{\text{irrad}}$ [Fig. 6(a)]. The average of the first five measurements thereafter can be taken as net change in OD for a given dose (i.e., *derivative method*) assuming ΔOD is calculated with respect to the initial OD of unirradiated film, as specified earlier. An alternative, *model method*, was used. In this method, the data were fitted linearly using the least squares, yielding three lines. These represent $\Delta OD(t)$ prior to irradiation, during irradiation, and after irradiation. The intercept of second and third linear fit was found, and was taken as the time of termination of irradiation [Fig. 6(b)]. With a justified assumption that the first fitted line is noise about $\Delta OD=0$, and the intercept between the first and second fitted lines is also zero within experimental error, the $\langle \Delta OD \rangle$ as given by the five points following termination of irradiation is what is reported as the ΔOD for a given radiation exposure. If the signal is not “zeroed” prior to each exposure (I_{0S} reset to the new amount of light intensity received, even though a dose might have been applied recently), and/or if the previously applied dose was large (~ 10 Gy), a slightly different approach can be taken. The ΔOD can be easily measured by using the intercept of first and second lines of fit [Fig. 6(c)]. That is, ΔOD for a given dose is then the $\langle \Delta OD \rangle$ measured immediately after intercept of second and third lines minus the $\langle \Delta OD \rangle$ measured immediately prior to intercept of first and second fit lines. This approach would be valid for other media where ΔOD versus dose is linear during exposure, and $(\delta(\Delta OD) / \delta t)_{\text{irrad}} > (\delta(\Delta OD) / \delta t)_{\text{post-irrad}}$, as seen for GafChromic MD-55 film.

As light-induced heating has the potential to induce local polymerization and contaminate the radiation-induced changes in OD,^{21,22(b)} it was important to make sure the power delivered to the sampled spot on the film was sufficiently low to avoid errors introduced by this process. The approximate power delivered to the film in the phantom was estimated using a lab-grade system [Newport 840-C power meter, Newport 818-SL detector, an Oriel Instruments Radiometric Power Supply, Oriel 250 W quartz-tungsten-halogen (QTH) lamp in Oriel Housing 66881, optical bandpass filter with 678 ± 10 nm full width at half maximum were used] that replicated the bandpass of the above-described LED but permitted greater accuracy in determining light transfer through the optical fiber, as the light coming out of delivery fiber was otherwise too dim to measure with

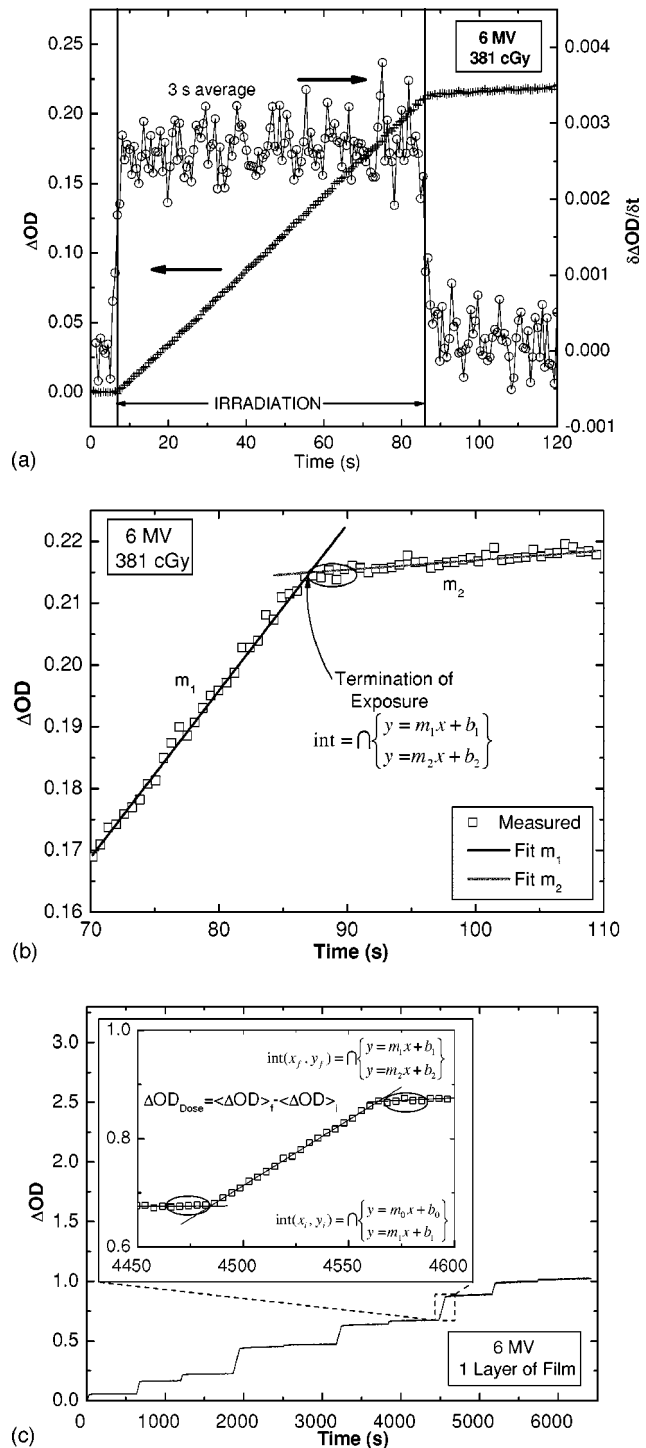


FIG. 6. (a) Change in optical density and rate of change in optical density for GafChromic MD-55 film as a function of time before, during, and after exposure to 381 cGy with 6 MV x rays. (b) Termination of exposure is taken as the intercept of the two fitted lines: the first line the corresponding to data obtained during exposure and the second line corresponding to data obtained after the end of exposure (\cap denotes intercept). (c) Change in optical density can be calculated for any exposure by subtracting initial ΔOD from final ΔOD .

other sources of light present in the room. The loss in power between the filtered QTH lamp and that delivered to film was then applied to the measured output of the LED operating at 30 mA. The LED, operating at 30 mA, outputs approxi-

mately 43 μW of light power resulting in approximately 7 nW at the end of the delivery fiber. The large power losses are mainly due to poor fiber-fiber coupling (simple SMA-to-SMA connectors are used), and inefficiency of coupling light out of 600 into a 50 μm fiber. However, since efficiency of the optical system is not the focus of this study, no improvements have been implemented.

The effect of this power on the film itself was measured using the above-noted equipment and setup for a film with a pre-existing OD corresponding to an exposure of approximately 4 Gy. The amount of light passing through phantom with a piece of GafChromic MD-55 film was recorded every 30 s over a period of 1 h. The light intensity at the reference channel was collected simultaneously, and the procedure was repeated six times. The slope of mean ΔOD in 670–680 nm range as a function of time was calculated for both signal and reference channel in the six trials. The results for signal and reference $\langle\Delta\text{OD}/s\rangle$ were found to be (-3 ± 5) and $(-2\pm 2)\times 10^{-6}$, respectively. Both are null results within error, and no significant difference between the two slopes was found (type I error of 5%, where type I error would occur if a hypothesis that the results are the same is rejected, even though it was true).³⁸

For exposures, the center of the GafChromic MD-55 film inside the phantom was located at the isocenter (100 cm from the source) of the linear accelerator (Varian 2100 EX), with the film plane parallel to the beam axis. A 10 cm \times 10 cm field of 6 MV x rays was used. The doses and dose rates reported here are those to a small volume of water in the center of the phantom. No corrections were applied to accommodate any perturbing effects associated with the small air-filled light transport cavities in the phantom and the fused silica optical fibers used [Fig. 4(d)]. The linear accelerator used for the experiments was calibrated using recommendations from TG21,³⁹ and its performance was monitored using an independent ion chamber⁴⁰ over the same period (60 days) during which the experiments were performed. The standard deviation in linear accelerator output over this time was found to be approximately 0.2%.

A. ΔOD of GafChromic MD-55 at various doses

Small “filmlets” (1 cm \times 1 cm) cut from a single sheet of GafChromic MD-55 film were inserted in the cylindrical phantom and exposed to single doses of 0, 24, 48, 95, 190, 286, or 381 cGy at 286 cGy/min, with three to six films repeated at each dose level. All spectra acquisitions were initiated 5–10 s prior to exposure. The acquisitions for films exposed to 381 cGy collected over a 1 h period. The spectra acquisitions for other films were collected over a period of 1–10 min. The ΔOD for each irradiation was calculated using the above-described *model method*. The results of these measurements formed the dose versus ΔOD calibration plot. Previously unexposed film from either the same sheet, or another sheet within the same batch, were then each irradiated to known doses in the range of 0–333 cGy (0, 67, 133, 200, 267, 333 cGy), with several individual films used per dose to evaluate precision. The calibration plot was applied

to the measured ΔOD to predict the applied radiation dose. All inferred doses for a given dose were averaged, and the values were compared to the applied doses.

The alternative method in which a pre-exposure calibration of known dose was applied for each filmlet, instead of batch calibration, was also investigated. Each filmlet was first exposed to 95 cGy at 286 cGy/min, and *sensitivity factor* in cGy per ΔOD unit was recorded. Eight 48 cGy exposures were then applied at 5 min intervals using the same dose rate to the same filmlet. Similarly, another piece of film was pre-exposed to 95 cGy, and then exposed to 190 cGy eight times. Changes in OD for each irradiation was calculated using the *model method*, and the inferred dose estimated using both the batch sensitivity factor and the individual pre-exposure sensitivity factor.

B. Sensitivity as a function of layer thickness

It has been previously shown that increasing the number of layers of GafChromic MD-55 increases the overall sensitivity.¹⁴ The same should hold true for the system presented here. Two more sets of filmlet holders were created with capacity to layer two or four pieces of film within the apparatus. Experiments were performed with one, two, and four stacked pieces of previously unexposed pieces of film with continuous exposure at a dose rate of 286 cGy/min to a maximum OD of 2.5. This was repeated three times. To estimate the sensitivity of the system, the ΔOD measured for the first ~ 1100 cGy in one- and two-layer setup was fit using the least mean squares. For the four-layer setup, the data for the first 700 cGy were considered. The slope of the linear regression line is taken as sensitivity of the system. The sensitivity for each of the one-, two-, and four-layer setups were compared.

C. ΔOD of GafChromic MD-55 at various dose rates

The influence of dose rate was explored over a range from 95 to 571 cGy/min. Filmlets were exposed to a specified

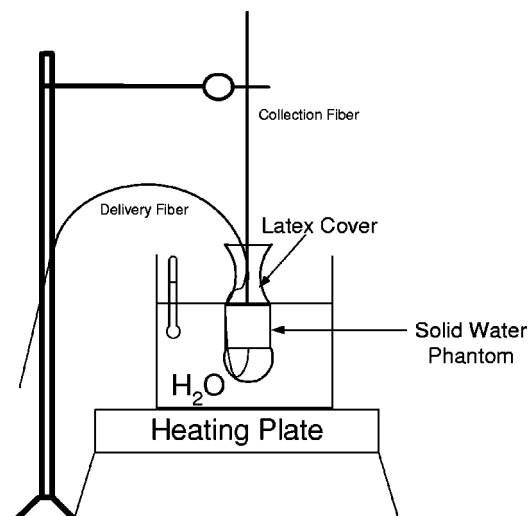


Fig. 7. Schematic of setup for temperature dependency experiments.

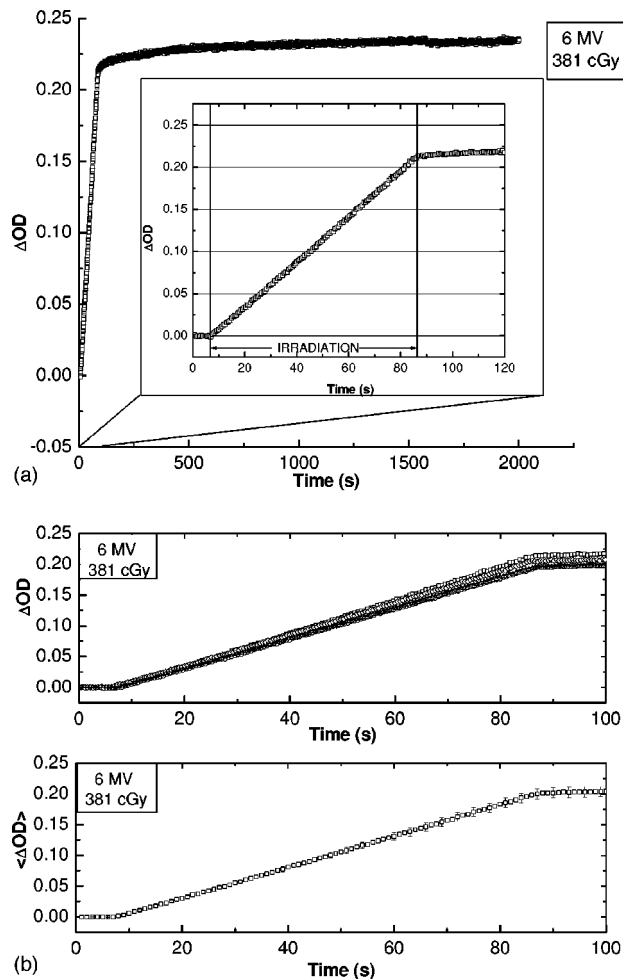


Fig. 8. (a) Change in optical density for GafChromic MD-55 exposed to 381 cGy with 6 MV x rays as a function of time. (b) Change in OD for five pieces of film, each exposed to 381 cGy with 6 MV x rays (at the dose rate of 286 cGy/min). The bottom plot illustrates the average of such measurements, with the error bar equivalent to σ (one standard deviation).

dose at three rates: at 95, 286, and at 571 cGy/min with approximately 5 min between irradiations. This was performed six times for the same dose, each time with a different permutation of dose rate and dose (of 24, 48, 95, 190, 286, or 381 cGy). The mean ΔOD and mean $\delta\Delta OD/\delta t$ were calculated for each dose at the three different dose rates, and the resulting values compared.

D. ΔOD dependency on temperature

To investigate the effect of temperature on the ΔOD , the phantom was placed into a waterproof cover (Endocavity Latex Ultrasound Transducer Cover, B-K Medical Systems Inc.) and submerged in a 1 L Pyrex™ beaker filled with ice water (Fig. 7). The beaker was positioned on a heating plate (Corning Glass Works PC 351). The center of the phantom was placed at isocenter and irradiated laterally by positioning the linear accelerator at 90°. The temperature reported is that of the water bath, which was controlled using the heating plate and monitored with a thermometer. Once the desired temperature was reached, the phantom and film within were

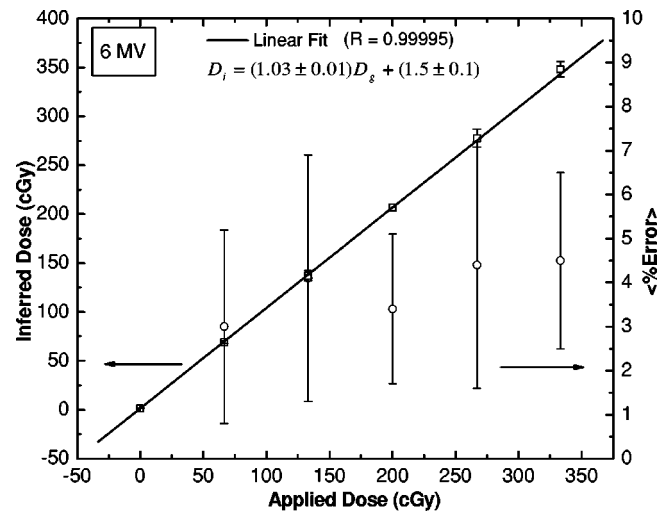


Fig. 9. Inferred dose using ΔOD measurements and calibration plot as a function of applied dose. The average percent error of inferred dose with respect to the applied dose is less than 5%. The error bars for both ΔOD and percent error data are equivalent to σ (one standard deviation).

given approximately 15 min to equilibrate. The spectra were collected during and after exposure, and ΔOD reported versus temperature are those immediately at the end of exposure.

E. Continuous versus pulsed irradiation

The influence of pulsed and continuous radiation on the *model method* was examined. With a single filmlet within the phantom, the device was positioned at 81.5 cm surface-to-axis distance under a Cobalt-60 treatment unit. Using a 10 cm \times 10 cm field, and a dose rate of 85 cGy/min, the film was exposed six times for a period of 1 min each, with approximately 5 min between exposures. A second single filmlet from the same sheet of film was exposed six times at an average dose rate of 85 cGy/min for a period of 1 min each on the linear accelerator. Using the *model method*, both the intra-exposure slope and ΔOD were calculated. The values were then compared between the two methods of irradiation.

III. RESULTS

A. ΔOD of GafChromic MD-55 at various doses

The ΔOD of film versus time for a dose of 381 cGy is shown in Fig. 8(a). The inter-exposure development appears to be logarithmic, while the ΔOD growth during exposure seems linear (see inset)—note the abrupt change in rates of ΔOD at the onset and completion of exposure. Figure 8(b) shows the $\Delta OD(t)$ for five pieces of film, each exposed to 381 cGy with 6 MV x rays. As the irradiation time and delivered dose increase, the deviation of ΔOD increases as well. Using the average ΔOD for each given dose in 0–4 Gy range, the calibration line was calculated to be

$$D(\text{cGy}) = (1 \pm 2) + (1863 \pm 22)\Delta OD.$$

This calibration equation and ΔOD of a new set of freshly irradiated films (applied doses of 0–333 cGy) were used to

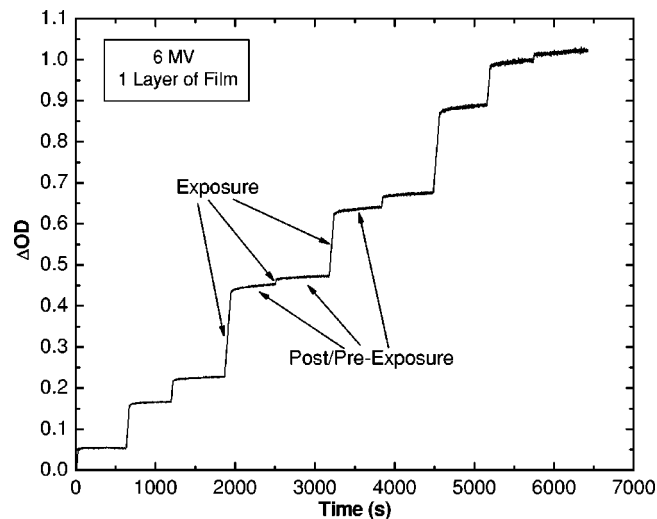


FIG. 10. Change in optical density for a piece of GafChromic MD-55 film during several exposures applied approximately 5 min apart.

calculate inferred dose, shown versus applied dose in Fig. 9. The linear fit yielded an intercept of 1.5 ± 0.1 cGy and a slope of 1.03 ± 0.01 (95% confidence, $r > 0.9999$). Figure 10 shows ΔOD versus time for a single piece of film, which was exposed multiple times. The sharp increases in ΔOD correspond to periods of intra-exposure to random doses, and the flatter regions are the data for inter-exposure. Using this ability of film to be exposed more than once and the pre-exposure calibration technique, inferred doses for 48 and 190 cGy irradiations are calculated. Table II compares the two methods of calculating inferred dose.

B. Sensitivity as a function of layer thickness

Figure 11 illustrates ΔOD as a function of dose for one, two and four layers of stacked filmlets, with the average sensitivity of (5.4 ± 0.2) , (10.9 ± 0.4) , and $(21.9 \pm 0.2) \times 10^{-4}$ $\Delta OD/cGy$, respectively. These correspond to an increase in sensitivity of 2.0 ± 0.1 , 2.01 ± 0.08 , and 4.1 ± 0.2 for $G_{\text{two layer}}:G_{\text{one layer}}$, $G_{\text{four layer}}:G_{\text{two layer}}$ and $G_{\text{four layer}}:G_{\text{one layer}}$ respectively, which are all within error of anticipated increases of two and four times.

C. ΔOD of GafChromic MD-55 at various dose rates

The average ΔOD measurements for a given dose at three different dose rates are shown in Fig. 12. Analysis of variance was performed on all measured ΔOD for a given dose. For 190 cGy, a statistically significant difference in ΔOD

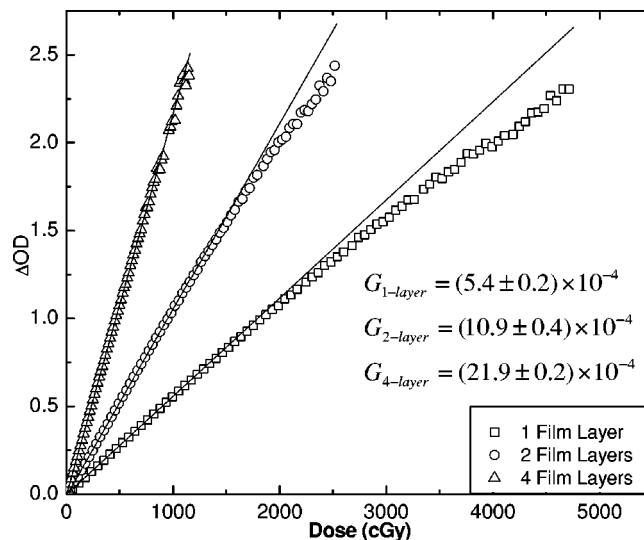


FIG. 11. Change in optical density as a function of dose for a system utilizing one, two, and four pieces of stacked film. G indicates signal gain, or the slope of the linear fit shown above.

measurements was found (type I error of 5%); however, no significant difference was found between the measurements obtained at different dose rates for type I error of 1%.³⁸ Nonetheless, a trend can already be seen in the ΔOD versus dose slopes calculated at each dose rate, where the deviations quoted are those for 95% confidence interval. The slopes of $\Delta OD/s$ as given by the *model method* calculation were also investigated (Fig. 13). They were $(8.7 \pm 0.3) \times 10^{-4}$, $(2.50 \pm 0.01) \times 10^{-3}$, and $(4.8 \pm 0.2) \times 10^{-3} s^{-1}$ for 95, 285, and 570 cGy/min, respectively. The slope ratios are 2.8 ± 0.2 , 2.0 ± 0.2 , and 5.6 ± 0.5 for $D_{285}:D_{95}$, $D_{570}:D_{285}$, and $D_{570}:D_{95}$, respectively. For a given dose rate, the slopes are within error of each other for doses in the 24–381 cGy range, even though the trend is for a higher slope estimate to appear at higher doses. An analysis of variance showed that there was a significant difference (type I error of 5%) between $\Delta OD/s$ estimates for different doses delivered at 95 and 571 cGy/min, but not at 286 cGy/min. At type I error of 1%, only $\Delta OD/s$ estimates for 95 cGy/min exhibited a significant difference between given doses.³⁸

D. ΔOD dependency on temperature

Using the 670–680 nm averaging window, ΔOD for a consistent dose was measured at each temperature. No effort was put into calculating the actual dose for this setup, but the exposures were all done at 300 monitor units/min for 1 min.

TABLE II. Comparison of inferred dose and percent error using calibration plot and pre-exposure calibration as methods of calculation.

| Dose (cGy) | Calibration plot | | | Pre-exposure calibration | | |
|------------|--|----------|------------|--|----------|------------|
| | $\langle \text{Dose}_i (\text{cGy}) \rangle$ | (%error) | (% error) | $\langle \text{Dose}_i (\text{cGy}) \rangle$ | (%error) | (% error) |
| 48 | 48 ± 2 | 0.52 | 3 ± 2 | 47 ± 2 | -0.54 | 3 ± 2 |
| 190 | 175 ± 7 | -7.8 | 8 ± 4 | 182 ± 7 | -4.5 | 4 ± 4 |

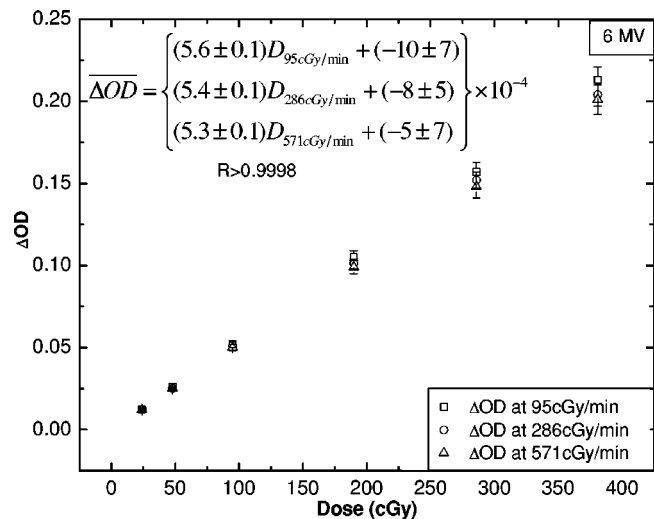


FIG. 12. Change in optical density as a function of dose for doses delivered at 95, 286, and 671 cGy/min.

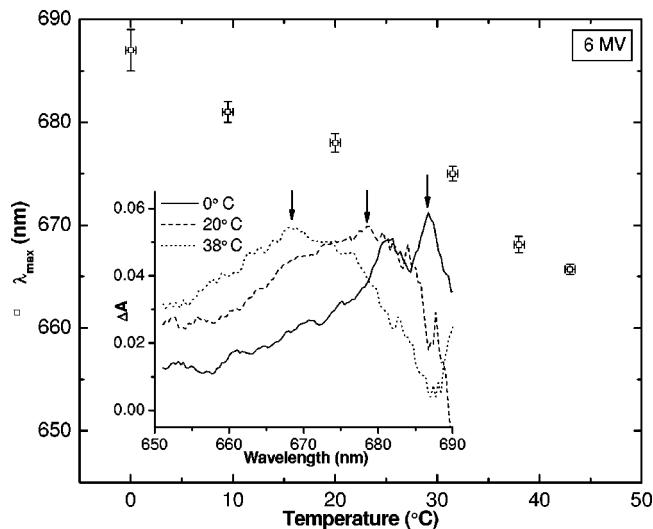


FIG. 14. Position of wavelength of maximum absorbance for GafChromic MD-55 as a function of irradiation/measurement temperature.

The mean ΔOD increases from 0.0331 ± 0.0008 at $0.0 \pm 0.5^\circ\text{C}$, to 0.0544 ± 0.0006 at $31.5 \pm 0.5^\circ\text{C}$, and then decreased to 0.041 ± 0.001 at $43.0 \pm 0.5^\circ\text{C}$. Figure 14 shows a decrease in λ_{max} to lower values with increasing temperature. To eliminate the temperature effect as purely that due to shifting of wavelength of maximum absorbance (λ_{max}), the average λ_{max} ($\langle \lambda_{\text{max}} \rangle$) was found for each irradiation at a given temperature, and the ΔOD was recalculated with the 10 nm averaging window approximately about this $\langle \lambda_{\text{max}} \rangle$ (Fig. 15). Averaging of ΔOD about λ_{max} instead of a fixed window increases measured $\langle \Delta OD \rangle$ for a given dose when λ_{max} is on the periphery or outside of the static averaging window.

E. Continuous versus pulsed irradiation

The mean regression slope (of the linear fit performed during application of *model method*) and ΔOD obtained for a film irradiated to 85 cGy at 85 cGy/min with Cobalt-60 are $(7.34 \pm 0.12) \times 10^{-4} \text{ s}^{-1}$ and 0.0447 ± 0.0012 , respectively. The mean regression slope and ΔOD obtained for a film irradiated to 85 cGy at 85 cGy/min with the linear accelerator are $(7.47 \pm 0.15) \times 10^{-4} \text{ s}^{-1}$ and 0.0447 ± 0.0012 , respectively. The ratio of the average slope obtained on a linear accelerator to average slope obtained on Cobalt-60 unit is 1.02 ± 0.03 . The ratio of the average ΔOD obtained on a linear accelerator to average ΔOD obtained on the Cobalt-60 unit is 1.00 ± 0.04 . Both ratios are within error of 1.00. Hence no difference in slope and ΔOD values between the two modes of dose delivery was found for a given dose delivered at the same dose rate.

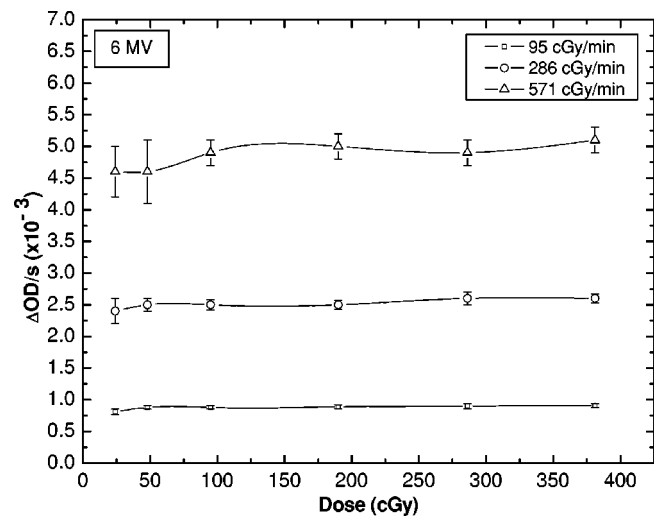


FIG. 13. Rate of change in optical density as given by the linear fit of data obtained during exposure as a function of applied dose, for doses delivered at 95, 286, and 571 cGy/min.

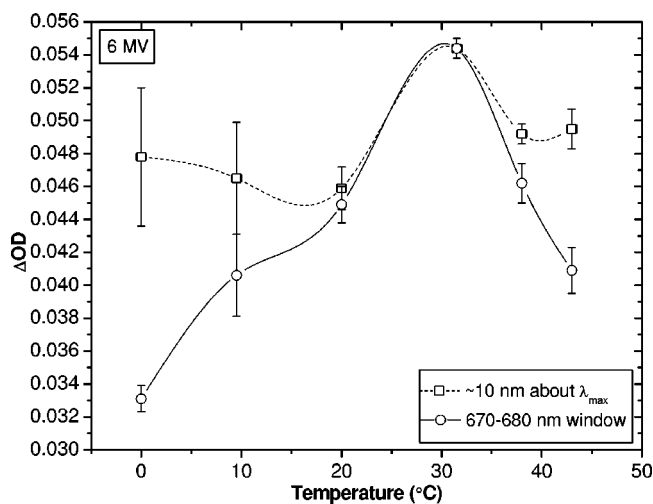


FIG. 15. Change in optical density for a given dose as a function of applied/measured temperature using both a constant spectral averaging window and a shifting spectral averaging window.

IV. DISCUSSION

The utilization of MD-55 for real-time, point-based dosimetry appears feasible based on the results presented here. There are a number of points that need to be raised with respect to these results: the relative stability of the sensitivity of the system (film in combination with optical path) is one of the significant sources of errors; the dynamic range for multiple-layer systems can be increased by modifying the light source and decreasing spectrophotometer noise; inter-exposure development introduces small errors to measurements for doses of ~ 2 Gy and above; temperature fluctuations in the range of 20–38 °C may be responsible for variation in ΔOD measurements of nearly 10%.

A. OD of GafChromic MD-55 at various doses

The sensitometric response difference $< 8\%$ from the mean within a single sheet, and $< 5\%$ from the mean between sheets of a single batch is expected [ISP Corp. product information]. The deviation of the ΔOD values seen for a single delivered dose can be easily explained by the possible sensitometric response variation inherent in this product.

While the fits performed in the calibration process are encouraging, there are some subtle elements. The fit of the inferred dose versus applied dose showed an intercept of 1.5 ± 0.1 and a slope of 1.03 ± 0.01 (95% confidence). Neither the intercept nor the slope is within error of the desired values of 0 and 1.00, respectively. One possible source of the intercept deviation is a systematic error introduced by the calculation procedure, where a nonzero dose is assumed to have been delivered, and it is not asked to distinguish true signal from noise. A more accurate procedure can be conceived which would include a minimum ΔOD threshold value, below which any signal is assumed to be merely noise. This threshold value would be based on the average of signal fluctuation expected for a given setup.

A closer look at percent error of each inferred dose with respect to the given dose shows a consistent overestimate, resulting in an average percent error of 3%–5% for each dose in question. The percent error is often within the 8% sensitometric variation of a single sheet of film. Although the 1 cm \times 1 cm pieces were picked randomly once cut, one half of the 5 in. \times 5 in. film was cut first for the calibration, and the second half was cut later for the testing of the method. This would suggest that the variation in sensitometric response of GafChromic MD-55 film is not random throughout the sheet, but rather increasing in a single direction, likely a by-product of the manufacturing process. The other source of errors may be the polarization effect of GafChromic MD-55 itself.¹⁸ Aside from placing the filmlets such that the same side of the film is always facing the interrogating light from the delivery fiber, no other efforts were made to position the long axis of the film at the same angle with respect to the collection fiber and spectrophotometer. If this position of the film is not reproduced exactly, variations in measured ΔOD will occur. To eliminate errors due to polarization effect of

GafChromic MD-55, the calibration plot and the measurements should be made with the long axis of the film always positioned in the same manner.

Table II shows the comparison between using a calibration plot and pre-exposure calibration to infer a dose. With the former, the inferred dose for 48 cGy tends to be overestimated on average, producing the mean percent error of $3 \pm 2\%$. While using the pre-exposure calibration produces the same mean percent error, on average the inferred doses are underestimated. The standard deviation of a measured ΔOD (average of five data points at the end of exposure) for a 48 cGy dose ranged between 0.0002 and 0.0007 units. Such low deviations in ΔOD illustrate that the amount of light getting to the spectrophotometer is sufficient to keep the noise reasonably low and close to the best possible precision of 0.0001 (using this 12 bit analog-to-digital converter). According to the calibration plot, this standard deviation of 0.0002–0.0007 corresponds to 1–2 cGy, or approximately 2%–4% for 48 cGy dose. Hence, it is not realistic that given such fluctuations in ΔOD for a single irradiation, we should expect errors lower than that. The deviations in ΔOD measurements for 190 cGy irradiations were 5×10^{-4} – 2×10^{-3} units, corresponding to a dose error of 2–5 cGy, or 1–3 % error. The observed errors are larger than expected for reasons that should be investigated further. Both methods underestimated the dose, but the pre-exposure calibration technique came closer to the given dose, and also decreased the mean percent error of the estimates by a factor of 2. This technique corrects some of the errors due to variation in film sensitivity and to polarization effect of the film itself.¹⁸ The pre-exposure technique described would also be useful to account for change in sensitivity as the dosimeter ages, since ΔOD increases with storage time,¹⁸ and response of film with dose depends on the total dose applied or ΔOD to date.¹⁵ For a clinical dosimeter using a sensitive medium such as GafChromic MD-55, this pre-exposure calibration would extend storage time after which the dosimeter can still be accurately used.

B. Sensitivity as a function of layer thickness

It was shown that increase in sensitivity occurred with increased thickness of ionizing-radiation sensitive layer. However, unless the light intensity, integration time, or number of averages taken is increased, the signal reaches the saturation level (spectrometer does not detect enough light to distinguish further increase in optical density, and ΔOD signal levels off) quicker for increased number of layers. A positive side effect of increasing layer thickness is also seen in reduced deviation of ΔOD measurements from linearity over the usable ΔOD range (before the optical system reaches saturation of $\Delta OD > 2.5$). It is known that GafChromic MD-55 film has a range of linear response for ΔOD versus dose, which depends on wavelength of measurement.^{9–13} Near the peak of maximum absorbance (~ 675 nm), this range is the shortest, partly due to shift of λ_{\max} with dose, and also due to loss of sensitivity as the polymer-to-monomer ratio within the crystal increases. This

effect is seen for the ΔOD versus dose curve for a single layer of film, but not seen for four layers of film. The simple explanation is that by the time saturation for this optical system is reached ($\Delta OD > 2.5$), the dose absorbed by each of the sensitive layers in the four-film system is approximately four times less than the dose absorbed by a single-film system at the same ΔOD value. Hence, the response of the film in four-film system to ionizing radiation dose does not deviate from linearity over the range of ΔOD used.

It is possible to increase the dynamic range of a multiple-layer system by using a lower noise, higher resolution spectrophotometer with a larger absorbance range, and by increasing the amount of incident light in the appropriate wavelength range. Implementation of a new light source must be done with caution, especially if continuous measurements are performed, as done for the experiments described here. Increasing the power of light source may induce changes in OD due to local heat polymerization from the light source itself.

C. ΔOD of GafChromic MD-55 at various dose rates

Each fraction of ionizing radiation causes a rapid change in OD of GafChromic MD-55 medium while local concentration of polymer is low, followed by a slow increase in OD due to increasing separation between adjacent monomers as polymerization proceeds and local concentration of polymers increases. If one waits 24–48 h after irradiation as recommended, then most of inter-exposure development will have completed. However, if the measurements are done immediately after the end of irradiation, the amount of inter-exposure development that has completed for a given dose depends on the time it took to give that dose, or the dose rate. Our results show that ΔOD measurements for a given dose at three different dose rates of 95, 286, and 571 cGy/min are indistinguishable (type I error of 1%) for all doses up to 381 cGy. Doses ≤ 95 cGy showed no dose-rate dependence (type I error of 5%), but those of ≥ 190 cGy either exhibited dose-rate dependence or were close to the critical F value. The F value is the average squared difference between means of sets, divided by the sampling variation expected; if the calculated F value is greater than the critical or expected F value for a total given number of data points, number of sets and type I error, then there is a statistically significant difference between the sets of data.³⁸ With our experimental setup and errors in ΔOD measurements, differences between sets of measurements done at different dose rates can be largely explained by fluctuations within the measured values themselves. At higher doses, the variation in ΔOD for various dose rates can introduce a substantial error.

The ratios of average $\Delta OD/s$ estimates are within error of the respective dose rates, showing that the rate of ΔOD increase during exposure is in fact proportional to the applied dose rate. The slopes ($\Delta OD/s$), as given by the linear fit of each curve during data processing, on average showed a higher slope estimate at higher doses. This is consistent with the presence of a slow-kinetics increase in OD toward the end of a single polymer chain. For a given dose rate, the

higher dose will have a longer irradiation period, and hence a greater inter-exposure development due to the first few fractions of the overall given dose. This extra ΔOD will result in a higher slope ($\Delta OD/s$) when linear fit is performed during calculation of ΔOD for this dose. To investigate how important the inter-exposure development from the first few fractions to the performance of the fitting algorithm is, an analysis of variance on $\Delta OD/s$ values for each dose rate was performed. Results showed that there was a significant difference (type I error 5%) between $\Delta OD/s$ estimates for different doses delivered at 95 and 571 cGy/min, but not at 286 cGy/min.³⁸ The discrepancy in $\Delta OD/s$ estimates for the lowest dose rate can be easily explained. The time difference between delivering 286 and 381 cGy is a full minute, and hence the larger the dose given, the greater ΔOD due to inter-exposure development has occurred. The linear regression performed during *model method* calculation will then take these higher values of ΔOD into account, giving a larger $\Delta OD/s$ estimate. The $\Delta OD/s$ estimates for highest dose rate may be out of error with each other due to fitting algorithm: the number of data points used in the fit at the highest dose rate is less (two or six times less) than the number of points used at the other dose-rates for the same given dose.

D. ΔOD dependency on temperature

Our results, which show an overall decrease in ΔOD for a given dose as one increases from approximately room temperature to over 40 °C, are consistent with previously published data. Part of the sharp decrease, once temperature reaches over 32 °C, and the large fluctuations within the temperature range are due to the position of λ_{\max} in the spectrum, and the choice of wavelength of interrogating light or spectral averaging window. The wavelength of maximum absorbance was found to decrease with temperature, and the λ_{\max} observed at 20 and 32 °C are similar to those reported earlier by Klassen.¹⁸ Averaging of ΔOD about λ_{\max} instead of a fixed window increases the measured $\langle \Delta OD \rangle$ for a given dose if λ_{\max} is on the periphery or outside of the static averaging window. However, even with λ_{\max} shift taken into account, an increase in ΔOD with temperature is seen between 0 and 30 °C, followed by a decrease in ΔOD . The latter can be explained by loss of monomer crystal structure that occurs as temperatures close to 60 °C are approached. The imperfect alignment of the monomers may alter unit cell parameters within the crystal and decrease the chance of polymerization.⁴¹

It is clear that changes in temperature of the dosimeter introduce new errors that are not accounted for by using either a calibration plot or a pre-exposure calibration done at a set range of wavelengths. Some of the errors can be eliminated if the averaging range for ΔOD measurements are done over 10 nm about the temperature-dependent λ_{\max} . The tracking of λ_{\max} might also reduce some of the error of using GafChromic MD-55 dosimeter after a long shelf life or after several large exposures, since λ_{\max} varies with storage time and total dose given.^{5,9,16,17,19} While ΔOD measurements can be made nearly independent of read-out temperature by us-

ing 632.8 nm,²⁰ changing the temperature during exposure and real-time readout introduces variations in chemical reaction rates that may ultimately lead to irreversible effects in ΔOD . The source of the remaining error, which can still be as high as 8%, is possibly due to loss of crystal structure upon temperature increase, which can affect sensitivity to ionizing radiation.^{23,24}

The aim for the dosimeter is to have broad applications, and often the temperature at which the dosimeter will be used cannot be known in advance. Requiring prior knowledge of the temperature in order to perform a pre-exposure calibration at that exact temperature significantly complicates its use and increases cost. A simpler dosimeter needs to have an insignificant temperature dependence over 20–38 °C range so that it can be calibrated at room temperature and require no use of correction factors.

E. Applications

Although the above-described apparatus and methods work sufficiently well for testing suitability of radiochromic media for real-time dosimetry, the system would not qualify as an *in vivo* dosimeter with its current design. The desired real-time *in vivo* dosimeter would meet all of the criteria discussed in Table I and would provide various improvements on existing dosimetry systems. One of the benefits of real-time dosimetry is the immediate access to dose information, unavailable with systems that require processing (e.g., thermo-luminescent dosimeters). The other significant improvement of the intended *in vivo* dosimeter is its near water-equivalency, which would eliminate the need for separate calibrations for energies that may be in use. This would allow the dosimeter to be used for various procedures, including verification of dose in areas that have unpredictable x-ray spectra (e.g., near small bony structures and air cavities that are relevant in some head and neck cancers), in the penumbra regions of large fields (where it would not overestimate dose due to low-energy over-response common in other dosimetry methods),^{10,42} in brachytherapy treatments with a variety of sources of different energies, during IGRT, fluoroscopy, and possibly others, while referring to a single calibration performed at a convenient energy of choice (such as Cobalt-60).

V. CONCLUSION

The change in optical density of GafChromic MD-55 as a function of time shows a rapid increase during exposure, with a rate that is proportional to applied dose rate. The end of exposure is marked by an abrupt decrease in rate of ΔOD , with the ΔOD increasing thereafter slowly with time, approaching a value that would typically be measured 24–48 h later and related to dose. It was found that ΔOD measured immediately at the end of exposure is proportional to dose in the tested range of 0–4 Gy. Performing such measurements can predict the applied dose immediately at the end of exposure with an average error of 5% for 0.67–3.33 Gy doses. Calibrating individually each dosimeter prior to its use can decrease the errors. To increase precision of low-dose predic-

tions, the sensitivity of the dosimeter can be proportionally increased by increasing the thickness of sensitive layer. For dose rates varying between 95 and 570 cGy/min, it was found that measurements of ΔOD immediately after the end of exposure did not depend on dose rate for low doses (≤ 100 cGy), typical of those delivered in a single beam during fractionated external beam radiation therapy. Higher doses (≥ 2 Gy) exhibited some dose-rate dependence. While GafChromic MD-55 appears to be suitable for real-time measurements of ionizing radiation dose, numerous issues remain. The ΔOD measurements performed immediately at the end of exposure exhibited significant temperature dependence in the clinically relevant range of 20–38 °C, which could not be corrected by shifting the spectral window of interest with the decreasing wavelength of maximum absorbance. Overall, this approach, which employs existing GafChromic MD-55, shows the promise of the novel readout configuration and method and has revealed some subtleties of the sensitive material in GafChromic MD-55 that were previously unreported.

ACKNOWLEDGMENTS

The authors wish to thank the following for their contribution: Yuen Wong and Brian Taylor, Robert Rothwell, Robert Rusnov, Dr. Robert Heaton, Cameron Chiarot, Dr. Douglas Moseley, Dr. Robert Weersink, and Photonics Research Ontario. This work was in part funded by National Institutes of Health / National Institute on Aging (R21/R33 AG19381) and by the Fidani Center for Radiation Physics.

^aElectronic mail: alex.rink@rmp.uhn.on.ca

¹International Commission on Radiation Units and Measurements (ICRU) Report No. 24, "Determination of absorbed dose in a patient irradiated by beams of x or gamma rays in radiotherapy procedures," 1976.

²N. Papanikolaou *et al.*, *Tissue Inhomogeneity Corrections for Megavoltage Photon Beams*, AAPM Report No. 85 (Medical Physics Publishing, Madison, 2004).

³A. Dutreix and A. Bridier, *Dosimetry for External Beams of Photon and Electron Radiation*, in *The Dosimetry of Ionizing Radiation*, Vol. 1, edited by K. R. Kase, B. E. Bjarngard, and F. H. Attix (Academic, Toronto, 1985).

⁴A. Miller and W. L. McLaughlin, "Absorbed dose distribution in a pulse radiolysis optical cell," *Int. J. Radiat. Phys. Chem.* **7**, 661–666 (1975).

⁵W. L. McLaughlin *et al.*, "Sensitometry of the response of a new radiochromic film dosimeter to gamma radiation and electron beams," *Nucl. Instrum. Methods Phys. Res. A* **302**, 165–176 (1991).

⁶W. L. McLaughlin *et al.*, "Novel radiochromic films for clinical dosimetry," *Radiat. Prot. Dosim.* **66**, 263–268 (1996).

⁷W. L. McLaughlin, M. Al-Sheikhly, D. F. Lewis, A. Kovacs, and L. Wojnarovits, "A Radiochromic Solid-state Polymerization Reaction," in *Irradiation of Polymers: Fundamentals and Technological Applications*, ACS Symposium Series No. 620 (ACS, Washington, DC, 1996).

⁸W. L. McLaughlin *et al.*, "The use of radiochromic detector for the determination of stereotactic radiosurgery dose characteristics," *Med. Phys.* **21**, 379–388 (1994).

⁹M. C. Saylor, T. T. Tamargo, and W. L. McLaughlin, "A thin film recording medium for use in food irradiation," *Radiat. Phys. Chem.* **31**, 529–536 (1988).

¹⁰P. J. Muench, A. S. Meigooni, R. Nath, and W. L. McLaughlin, "Photon energy dependence of the sensitivity of radiochromic film and comparison

- with silver halide film and LiF TLDs used for brachytherapy dosimetry," *Med. Phys.* **18**, 769–775 (1991).
- ¹¹S. Chiu-Tsao, A. Zerda, J. Lin, and J. H. Kim, "High-sensitivity GafChromic film dosimetry for ¹²⁵I seed," *Med. Phys.* **21**, 651–657 (1994).
- ¹²L. E. Reinstein and G. R. Gluckman, "Comparison of dose response of radiochromic film measured with He-Ne laser, broadband, and filtered light densitometers," *Med. Phys.* **24**, 1531–1533 (1997).
- ¹³L. E. Reinstein, G. R. Gluckman, and H. I. Amols, "Predicting optical densitometer response as a function of light source characteristics for radiochromic film dosimetry," *Med. Phys.* **24**, 1935–1942 (1997).
- ¹⁴T. Cheung, M. J. Butson, and P. K. N. Yu, "Use of multiple layers of GafChromic film to increase sensitivity," *Phys. Med. Biol.* **46**, N235–N240 (2001).
- ¹⁵I. Ali, C. Costescu, M. Vicic, J. F. Dempsey, and J. F. Williamson, "Dependence of radiochromic film optical density post-exposure kinetics on dose and dose fractionation," *Med. Phys.* **30**, 1958–1967 (2003).
- ¹⁶R. D. H. Chu *et al.*, "GafChromic dosimetry media: A new high dose, thin film routine dosimeter and dose mapping tool," *Radiat. Phys. Chem.* **35**, 767–773 (1990).
- ¹⁷A. Mack *et al.*, "High precision film dosimetry with GafChromic® films for quality assurance especially when using small fields," *Med. Phys.* **30**, 2399–2409 (2003).
- ¹⁸N. V. Klassen, L. van der Zwan, and J. Cygler, "GafChromic MD-55: Investigated as a precision dosimeter," *Med. Phys.* **24**, 1924–1934 (1997).
- ¹⁹A. S. Meigooni, M. F. Sanders, G. S. Ibbott, and S. R. Szeglin, "Dosimetric characteristics of an improved radiochromic film," *Med. Phys.* **23**, 1883–1888 (1996).
- ²⁰L. E. Reinstein and G. R. Gluckman, "Optical density dependence on postirradiation temperature and time for MD-55-2 type radiochromic film," *Med. Phys.* **26**, 478–484 (1999).
- ²¹P. R. Sullivan, B. F. Hasson, C. H. Grossman, and L. D. Simpson, "Optical density changes of GafChromic MD-55 film resulting from laser light exposure at wavelengths of 671 nm and 633 nm," *Med. Phys.* **27**, 245–251 (2000).
- ²²MSDS, prepared by ISP Corp., 01/11/2002; Dr. David Lewis, ISP Corp. (private communication).
- ²³R. H. Baughman, "Solid-state synthesis of large polymer single crystals," *J. Polym. Sci., Part B: Polym. Phys.* **12**, 1511–1535 (1974).
- ²⁴R. H. Baughman and K. C. Yee, "Solid-state polymerization of linear and cyclic acetylenes," *J. Polym. Sci. A* **13**, 219–239 (1978).
- ²⁵J. Guillet, "Photopolymerization," in *Polymer Photophysics and Photochemistry: An Introduction to the Study of Photoprocesses in Macromolecules* (Cambridge University Press, New York, 1985).
- ²⁶H. Sixl, "Electronic structures of conjugated polydiacetylene oligomer molecules," in *Electronic Properties of Polymers and Related Compounds*, edited by H. Kuzmany, M. Mehring, and S. Roth (Springer, Heidelberg, 1985).
- ²⁷D. Bloor, L. Koski, G. C. Stevens, F. H. Preston, and D. J. Ando, "Solid state polymerization of bis-(*p*-toluene sulphonate) of 2,4-hexadiyne-1,6-diol," *J. Mater. Sci.* **10**, 1678–1688 (1975).
- ²⁸H. Sixl and R. Warta, "Excitons and polarons in polyconjugated diacetylene molecules," in Ref. 26.
- ²⁹J. Tsibouklis *et al.*, "Pentacosanoic Acid/Henicosanoic Acid/2,4-diaminobenzene alternate-layer Langmuir-Blodgett films: Synthesis, polymerization and electrical properties," *J. Mater. Chem.* **3**, 97–104 (1993).
- ³⁰G. Solomons and C. Fryhle, *Organic Chemistry*, 7th ed. (Wiley, Toronto, 2002).
- ³¹J. H. O'Donnell and D. F. Sangster, *Principles of Radiation Chemistry* (Arnold, London, 1970).
- ³²A. L. Huston *et al.*, "Remote optical fiber dosimetry," *Nucl. Instrum. Methods Phys. Res. B* **184**, 55–67 (2001).
- ³³K. H. Becks, J. Drees, K. Goldmann, I. M. Gregor, and M. Heintz, "A multichannel dosimeter based on scintillating fibers for medical applications," *Nucl. Instrum. Methods Phys. Res. A* **454**, 147–151 (2000).
- ³⁴H. Bueker and F. W. Haesing, "Fiber-optic radiation sensors," *Proc. SPIE* **2425**, 106–114 (1994).
- ³⁵S. Gripp, F. W. Haesing, H. Bueker, and G. Schmitt, "Clinical *in vivo* dosimetry using optical fibers," *Radiat. Oncol. Invest.* **6**, 142–149 (1998).
- ³⁶M. J. Day and W. G. Pitchford, "The normalized peak scatter factor and normalized scatter functions for high energy photon beams," in *British Journal of Radiology Supplement 25: Central Axis Depth Dose Data for Use in Radiotherapy: 1996* (The British Institute of Radiology, London, 1996).
- ³⁷F. Fusi, L. Mercatelli, G. Marconi, G. Cuttone, and G. Romano, "Optical characterization of radiochromic film by total reflectance and transmittance measurements," *Med. Phys.* **31**, 2147–2154 (2004).
- ³⁸J. S. Milton and J. C. Arnold, *Introduction to Probability and Statistics: Principles and Applications for Engineering and the Computing Sciences*, 2nd ed. (McGraw-Hill, Toronto, 1990).
- ³⁹R. J. Schulz *et al.*, "A protocol for the determination of absorbed dose from high-energy photon and electron beams," *Med. Phys.* **10**, 741–771 (1983).
- ⁴⁰E. Martell, D. Galbraith, P. Munro, J. A. Rawlinson, and W. B. Taylor, "A flatness and calibration monitor for accelerator photon and electron beams," *Int. J. Radiat. Oncol., Biol., Phys.* **12**, 271–275 (1986).
- ⁴¹R. H. Baughman, "Solid-state reaction kinetics in single-phase polymerizations," *J. Chem. Phys.* **68**, 3110–3121 (1978).
- ⁴²B. Wang, C. Kim, and X. G. Xu, "Monte Carlo modeling of high-sensitivity MOSFET dosimeter for low- and medium-energy photon sources," *Med. Phys.* **31**, 1003–1008 (2004).